Journal of Inorganic and Organometallic Polymers and Materials
https://doi.org/10.1007/s10904-024-03226-w

RESEARCH

Biogenic Production of Silver Nanoparticles Using *Neocosmospora Solani* Endophytic Fungal Extract: Their In Vitro Antibacterial and Anticancer Properties

Kistu Singh Nongthombam[1] · Surendirakumar Kannaiah[1,2] · Prabhu Raju[3] · Lakshmanan Govindan[4] · Shyamkesho Singh Mutum[1] · Radha Raman Pandey[1]

Received: 3 May 2024 / Accepted: 21 June 2024
© The Author(s), under exclusive licence to Springer Science+Business Media, LLC, part of Springer Nature 2024

Abstract

The biogenic synthesis of nanomaterials has great advantages, biocompatible, and valuable material production. In this study, we demonstrated a sustainable and biocompatible approach for the synthesis of Ag nanoparticles (Ag NPs) using the endophytic fungi *Neocosmospora solani* (NS) extract isolated from the *Anaphalis contorta* stem. The anticancer and antibacterial potential of bioactive NS mediated AgNPs was evaluated by in vitro studies. The physicochemical characteristics of synthesized NS-AgNPs were systematically investigated by UV-vis, XRD, FTIR, FE-SEM, DLS and Zeta potential analyzer. In details, UV-visible spectroscopy confirmed the presence of biosynthesized NS-AgNPs at 432 nm, while XRD analysis confirmed their crystal nature. The FTIR spectrum confirmed the presence of functional groups in biomolecules that act as a capping agent for the nanoparticles. SEM was used to evaluate the shape of AgNPs. Dynamic light scattering (DLS) indicated that the average particle size is 362.3 nm, a zeta potential was −0.168 mV with a single peak. The biosystem technique produced stable AgNPs up to 2 months following synthesis. In addition, the NS-AgNPs were exposed to excellent antibacterial efficacy against human pathogenic bacterial strains. The results of the anticancer assessment of NS-AgNPs against A549 lung cancer cells revealed that the dose-dependent cytotoxic and morphological changes have been reported in both AO/EB and Hoechst's staining assays. In the future, it might be an excellent antibiotic and anticancer material for biomedical applications.

Keywords Anticancer · Antibacterial · Biocompatibility · Cell viability · Silver nanoparticles · Fungi

1 Introduction

Cancer is a leading cause of human death in developing countries. It is a second major reason for death of adults in rural and urban India. Oral cancers occur in both men and women Worldwide [1, 2]. It is the fifth most common cancer after cervical, breast, stomach, and lung cancers [3]. The existence of metals from nature is widely fabricated in nanostructures. Silver nanoparticles have great attention in biomedical research, due to their unique properties [4]. Unlike physical and chemical approaches, the green synthesis technique is eco-friendly and inexpensive, making it a promising method. Plant extracts are used for the reduction silver nitrate to form silver nanoparticles. Among the bioresources, microbes-mediated nanoparticle synthesis is the most reliable technique [5]. Secondary metabolites and microbial enzymes entertain a promising role in

✉ Surendirakumar Kannaiah
surenderpbt@gmail.com

[1] Department of Life Sciences (Botany), Manipur University, Canchipur, Imphal 795 003, Manipur, India

[2] Department of Microbiology, JJ College of Arts and Science (Autonomous), (Affiliated to Bharathidasan University, Tiruchirappalli), Pudukkottai 622 422, Tamilnadu, India

[3] Department of Biotechnology, JJ College of Arts and Science (Autonomous), (Affiliated to Bharathidasan University, Tiruchirappalli), Pudukkottai 622 422, Tamilnadu, India

[4] Department of Anatomy, Saveetha Medical College and Hospital, Saveetha Institute of Medical and Technical Sciences, Chennai 602 105, Tamilnadu, India

Published online: 16 September 2024

the transformation of metal ions into nanostructures. It plays a significant role in industrial and biomedical fields like electronics, cosmetics, antitumor, wound healing and antimicrobial applications [6]. Recently, the disadvantages of nanoparticle synthesis in chemical methods are the need for high-energy equipment and particle contamination. The surfactants and solvents are highly harmful to the ecosystem and lead to human diseases. Fungal endophytes have been considered as bio-factory for producing metal nanoparticles for agricultural and biomedical applications. These fungi colonize plants intra- and intercellular tissues, forming a symbiotic connection [7]. The endophytes may benefit plant health and development through a variety of mechanisms, including the secretion of antimicrobial compounds and the production of growth-enhancing metabolites. Endophytic fungi residing inside plant tissues can produce nanoparticles [8]. Endophytes may withstand and/or collect metals in the environment to relieve toxicity and stress in the host plant and promote their competitive adaption over other niche microbes. The capacity of endophytes to detoxify metals can be used to synthesize metal-based nanoparticles through extracellular and intracellular mechanisms [9]. It will reduce the cost effectiveness of nanomaterial synthesis and the toxicity of ecosystems. The presence of phytochemicals can enhance the biological potential of nanomaterials against human pathogens and cancer cells [10].

On the contrary, *Anaphalis contorta* is an erect plant, and its fresh leaves are used to treat wounds [11, 12]. The plant pastes are also used for the treatment of cough. The oil extracted from the *Anaphalis contorta* leaves effectively inhibits the disease-causing human pathogenic bacteria and fungi [13]. Recently, studies exhibited that fungal cultures were used for the synthesis of nanomaterials in an eco-friendly manner. The presence of proteins, phenols and flavonoids are important phytochemicals for metal ion reduction [14]. Unfortunately, only a few endophytic fungi have been reported in Ag nanoparticles synthesis using *Aspergillus clavatus, Epicoccum nigrum, Penicillium* sp., and *Fusarium solani*. More than 80% of herbal medications, phytochemicals derived from endophytic fungi and medicinal plants [15–18]. In this study, endophytic fungi, *Neocosmospora solani*, isolated from the stem of *Anaphalis contorta*, was used to synthesize Ag nanoparticles. The physicochemical characteristics were examined by various spectroscopic and microscopic techniques. The current findings represent the first evidence of the biological activity of silver nanoparticles generated by *Neocosmospora solani*. It might be an excellent biocompatible nanomaterial for biomedical applications.

2 Materials and Methods

2.1 Materials

Fetal bovine serum (FBS), propidium iodide (PI), agarose, propidium iodide (PI), RNase, triton X-100 and buffered saline (10X) were purchased from Gibco Invitrogen Life Technologies. Silver nitrate, sodium bicarbonate, thiazolyl tetrazolium bromide, dimethyl sulfoxide were purchased from Sigma Aldrich, USA. Dulbecco's modified Eagle's medium, streptomycin trypsin, penicillin, EDTA and methanol were purchased from HiMedia, India. Human lung cancer A549 cell lines were obtained from NCCS, Pune, India.

2.2 Isolation of the Endophytic Fungus

Healthy *Anaphalis contorta* stems were collected from Manipur [12]. Endophyte fungal isolation was based on a prior investigation by [19] with some changes. The collected stems were washed thoroughly in sterile DD water and cut into small fragments (1 cm). The stem fragments were sterilized by 4% sodium hypochlorite and 70% ethanol solutions for 10 min. After the surface sterilization stem pieces were washed twice with sterile DD water. The surface sterilized stem fragments are dried for 5 min using filter paper to remove moisture and transferred into a Petri dish with PDA (potato dextrose agar). To prevent bacterial contamination, 150 mg L of streptomycin sulfate was added to the agar medium. Further, plates were incubated for 7 days at 28 °C. The new fungal colonies were separated from the stem tips and transferred to new PDA plates were stored at 4 °C for further studies [19].

2.3 Identification of Endophyte Fungi

Morphological characteristics were identified with the assistance of the NFCCI (National Fungal Culture Collection of India, Pune, India. The results revealed that, the isolated endophytic fungi (Strain ID: S8), *Neocosmospora solani* (Mart.) L. (Accession no. NFCCI 522) belongs to the order Sordariomycetes and the family Nectriaceae.

2.4 Biosynthesis of NS-AgNPs

The endophytic fungi *Neocosmospora solani* (NS) (NFCCI 522) was inoculated in 200 mL of PDB (potato dextrose broth) and incubated at 28 ± 2 °C for 72 h in a rotary shaker at 120 rpm speed. After that, the biomass was collected and filtered through Whatman filter paper No.1. Excess mount medium washed with sterile DD water for removal of unwanted media components. The fungal biomass (10 g) was suspended in 250 mL flask with 100 mL of DD water

and agitated at 120 rpm for 48 h at 28 ± 2 °C. Following the incubation period, fungal filtrate was separated by using Whatman filter paper. This biomass filtrate was used for NS-AgNPs synthesis. About 10 mL of clear fungal solution (i.e. *Neocosmospora solani*- NS extract) was treated with 90 mL of (1 mM) silver nitrate solution and incubated overnight in the dark. The color of the silver nitrate solution shifted from colorless to orange brown. The color change precursor solution indicates the emergence of silver nanoparticles [16, 20]. The synthesized Ag nanoparticles was separated by centrifugation for 20 min at 10,000 rpm speed. The pellets were dried at 60 °C for 24 h. Finally, pure silver nanoparticles were kept at 4 °C for future research.

2.5 Characterization of NS-Ag NPs

Synthesis of *N. solani* (NS) mediated Ag nanoparticles (NS-AgNPs) was identified by the visual observation of a color change from transparent solution to orange brown color colloid. UV-visible spectroscopy (UV-3600 Shimadzu, Japan) was used to identify the formation of AgNPs [14]. The powder XRD technique (XRD6000, Shimadzu) was used to examine the crystalline structure of AgNPs. X-ray diffraction was recorded in the 2θ range of 10–80 degrees [16]. The presence of functional groups of AgNPs was identified by using Shimadzu 8400 FTIR Spectrophotometer at 4000–400 cm^{-1} range. Field Emission-Scanning electron microscopy (FE-SEM) was used to evaluate the surface morphology of Ag NPs. Furthermore, the stability and size distribution of synthesized NS-AgNPs was determined by using a Zeta analyzer and DLS (Dynamic light scattering) (Malvern Instruments Ltd., UK) [20–23]. The average crystalline size of NS-AgNPs was calculated by using the Scherrer Equation: $Dp = (0.94 \times \lambda) / (\beta \times \cos\theta)$.

Where, Dp = Average Crystallite size, β = Line broadening in radians, θ = Bragg angle, λ = X-Ray wavelength.

2.6 Antibacterial Assay

The antibacterial effectiveness of produced NS-AgNPs was investigated using the agar well diffusion method [19] against the human pathogens, *Staphylococcus aureus*, *Salmonella typhi, Escherichia coli* and *Bacillus subtilis* obtained from RIMS (Regional Institute of Medical Sciences), Imphal. The bacterial strains (10^7 cells mL) were sub-cultured in a nutrient broth (NB) medium in an overnight culture. After the subculture the bacterial strain was swabbed uniformly onto the agar plates using sterile cotton swab, various doses of (20, 40, and 60 µg mL) of NS-AgNPs were loaded into each well. The stranded antibiotic Streptomycin sulfate was considered as a positive control. Nanoparticle-treated plates were incubated for 24 h at 37 °C. After 24 h of post-exposure, the zone of inhibition (mm) was calculated by zone scale [22].

2.7 Cytotoxicity Assessment Using MTT Assay

A549 lung cancer cells were sub-cultured in DME medium 10% fetal bovine serum with 100 µg mL of streptomycin and penicillin [24]. The cells were maintained in a tissue culture flask in a CO_2 incubator under 5% CO_2 flow at 37 °C. After the ~90% of cell confluency, they were trypsinized with trypsin (0.05%) and EDTA solution. The cells were treated with various doses (20–100 µg mL) of NS-AgNPs. Additionally, the treated cells were stained with 50 µL of MTT solution, and again incubated for 4 h at 37 °C. An excess amount of MTT stains were separated by DMSO. The absorbance of media was measured by using ELISA plate reader at 570 nm absorbance. The total number of cell viability was calculated using the following equation: % of cell viability = (OD of treated sample / OD of control sample) × 100 [21, 22].

2.8 Assessment of Apoptosis

The AO/EtBr dual staining approach was utilized to examine the apoptosis of NS-AgNPs treated A549 cells [22]. The cells were treated with an IC_{50} concentration based on the MTT cytotoxicity assay [24]. Treated A549 cells were incubated at 37 °C for 4 h under 5% of CO_2 flow. The cells were washed with PBS solution and placed on the glass slides. Then, the 10 µL of AO/EtBr stains were added and incubated for another 10 min for stain fixation. The surplus floating stain was removed by washing twice with PBS solution. A fluorescent microscope was used to obtain cellular pictures (Nikon ECLIPSE, Ti-E, Japan).

2.9 Assessment of Nuclear Damage by Hoechst 33,342 Staining

The cytomorphological changes and nuclear damages of A549 cells were identified by Hoechst staining technique according to the previous method [25]. Cells were treated with IC_{50} concentration of NS-AgNPs. Cells were subjected to Hoechst staining for 15 min at the concentration of 0.5 mg mL. The cells were then rinsed with 5 mL of PBS buffer. Cells were observed using a fluorescent microscope with an emission wavelength of 420 nm and an excitation wavelength of 365 nm. More than one hundred cells were chosen at random, and the percentages of living and apoptotic cells were calculated using image J 2.4 software [25].

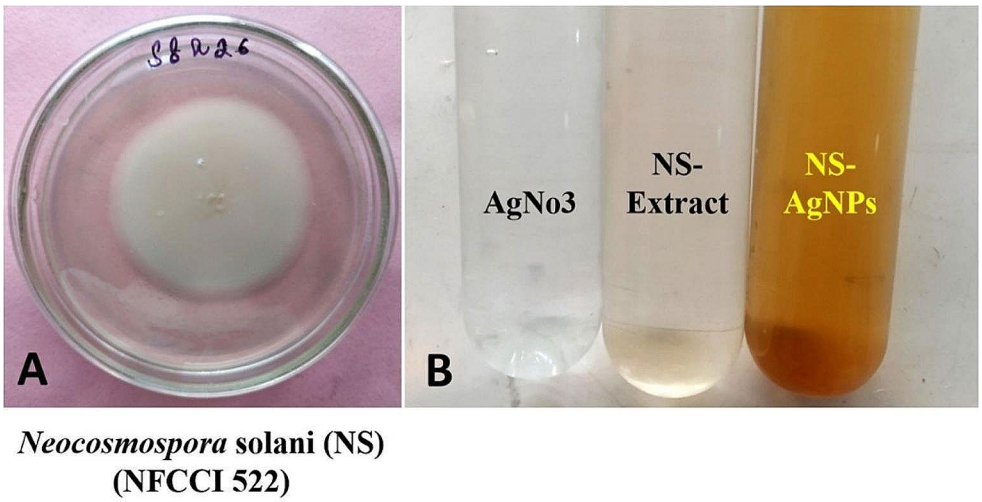

Fig. 1 (**A**) Culture of *Neocosmospora solani* (NS), (**B**) biosynthesis of silver nanoparticles

2.10 Statistical Analysis

All experimental data were represented as mean ± standard deviation. The statistical significance of all tests was set at $*p < 0.05$. All the spectral graphs were prepared by Prism.8.0 software. The XRD, FTIR, and UV graphs were prepared by OriginPro.9.0 software.

3 Results and Discussion

3.1 Isolation and Identification of Fungal Endophyte

In this work, 24 endophytic fungal morphotypes from twelve taxa were discovered and deposited in NFCCI (data not shown). *Penicillium* had the most species (6), followed by *Aspergillus* (4), *Trichoderma* (4) and *Fusarium* (3). *Cladosporium* and *Phoma* have two species each. However, just one species was recovered from *Alternaria*, *Epicoccum* and *Neocosmospora*. Among all these strains, S8 was the unique, with a isolation frequency (%IF) of 14.52% (data not shown) and randomly selected for further investigations. The studied endophytic fungal colony had dense and white villous mycelia and have a faster growth rate (10.5 ± 0.20 mm per day) on PDA medium. The fungal isolate (S8) was identified as *Neocosmospora solani* using morphological traits and confirmed by NFCCI. The NFCCI accession numbers obtained were "NFCCI 522" which belongs to the order Sordariomycetes and the family Nectriaceae. In another study, the fungal endophytes isolated from the medicinal plant *Anaphalis contorta* produced the natural bioactive compound and its secondary metabolites showed potent antibacterial activity against *Bacillus subtilis*, *E. coli* and *Staphylococcus* sp. [11, 12].

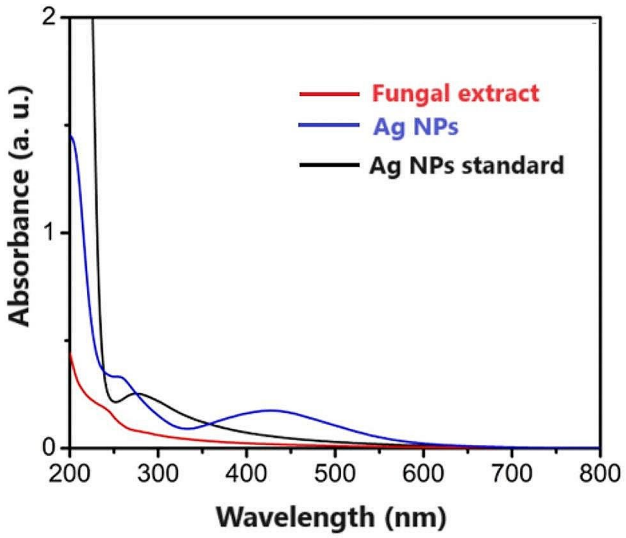

Fig. 2 UV-vis spectrum of synthesized silver nanoparticle using *Neocosmospora solani* extract

3.2 UV-Vis and XRD Analysis

The color changes of the Ag solution from white to orange brown indicates the formation of Ag nanoparticles (NPs) due to the reduction of nitrate from the precursor solution (Fig. 1) [22]. The metal-chelating ability of *N. solani* (NS) extract plays a prominent role in NPs synthesis. The trapping and enzymatic reduction ability of fungal cells effectively reduces the Ag + ions in silver nitrate solution. The UV-Vis spectra of *N. solani* mediated Ag nanoparticles (NS-AgNPs) shown in Fig. 2. The characteristic absorbance of synthesized silver nanoparticles shows a sharp peak at range of 432 nm. No absorbance occurs in the fungal extract. Previous research [5, 21] suggests that biogenic synthesis of silver nanoparticles has a lower toxicity for people.

The crystalline structure of fabricated NS-AgNPs was confirmed by powder XRD analysis [8]. The X-ray diffraction peaks at around 33.03º, 46.17º, 58.1º and 76.08º confirming the crystal planes of (111), (200), (220) and (311) matched with JCPDS: 04-0783 cubic centered crystal structure of silver nanoparticles (Fig. 3). The Powder XRD patterns indicate that the silver nanoparticles were fabricated by green method and observed in aggregated spherical Ag nanoparticles with a mean size of 150 nm was noticed in a scanning electron microscope (Fig. 5) [22]. XRD analysis of NS-AgNPs showed intensive peaks corresponding to (111), (200) and (220) based on Bragg's reflection, and the Ag nanoparticle structure is found to be FCC [9, 24]. Previous publications are remarkably similar to our findings [26].

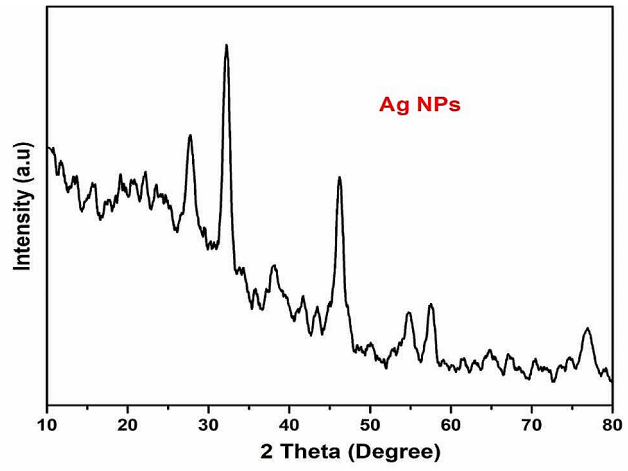

Fig. 3 Powder XRD spectrum of NS mediated AgNPs.

3.3 FTIR and FE-SEM Analysis

FT-IR spectrum of NS-AgNPs indicates that the interaction of biomolecules showed intensive peaks at 3431 cm^{-1} represents the O–H stretching vibration of alcohols and phenol. The peak at around 2921 cm^{-1} is attributes he O–H stretching of carboxylic acid. The small peak at 2851 cm^{-1} range indicates the O–H bending vibration of water molecules. The peaks at around 2041, 1384 and 1307 cm^{-1} correspond to C = C, C–H and C–O stretching of alcohol, ester, and ether functional groups [18, 21] (Fig. 4). FE-SEM images were captured at different magnifications. The FE-SEM images showed highly dense agglomerated nanoparticles [21]. The combination of fungal extract and silver which affected the crystallinity of synthesized Ag nanoparticles (Fig. 5) [22].

3.4 DLS and Zeta Potential Analysis

The DLS data (NS-Ag NPs) showed that the Z-average (nm) was 362.3 nm with a PdI value of 0.873 (Fig. 6). The acquired peak suggested that the quality of the produced silver nanoparticles was satisfactory. The size of nanoparticles differed between SEM and DLS, which could explain particle aggregation [21]. Surface charge of the nanomaterials acts as a determining factor in the stability and cellular responses [24]. In an aqueous solution of Ag solution exhibits uniform dispersion with a high level of solubility,

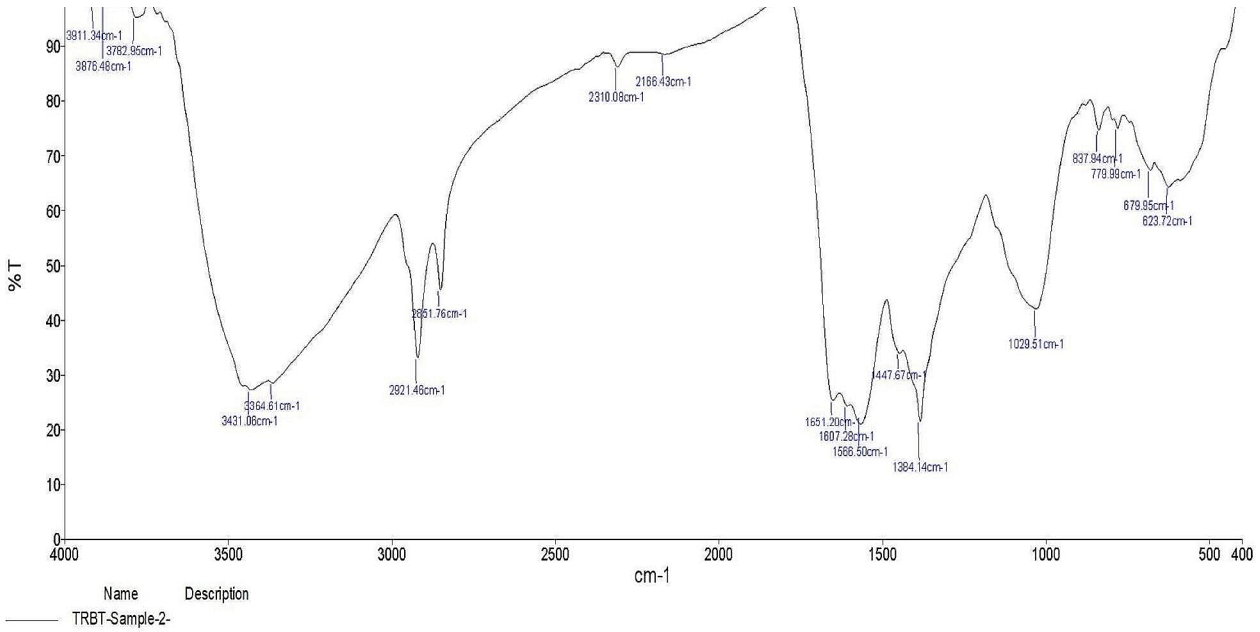

Fig. 4 FTIR spectrum of NS-AgNPs

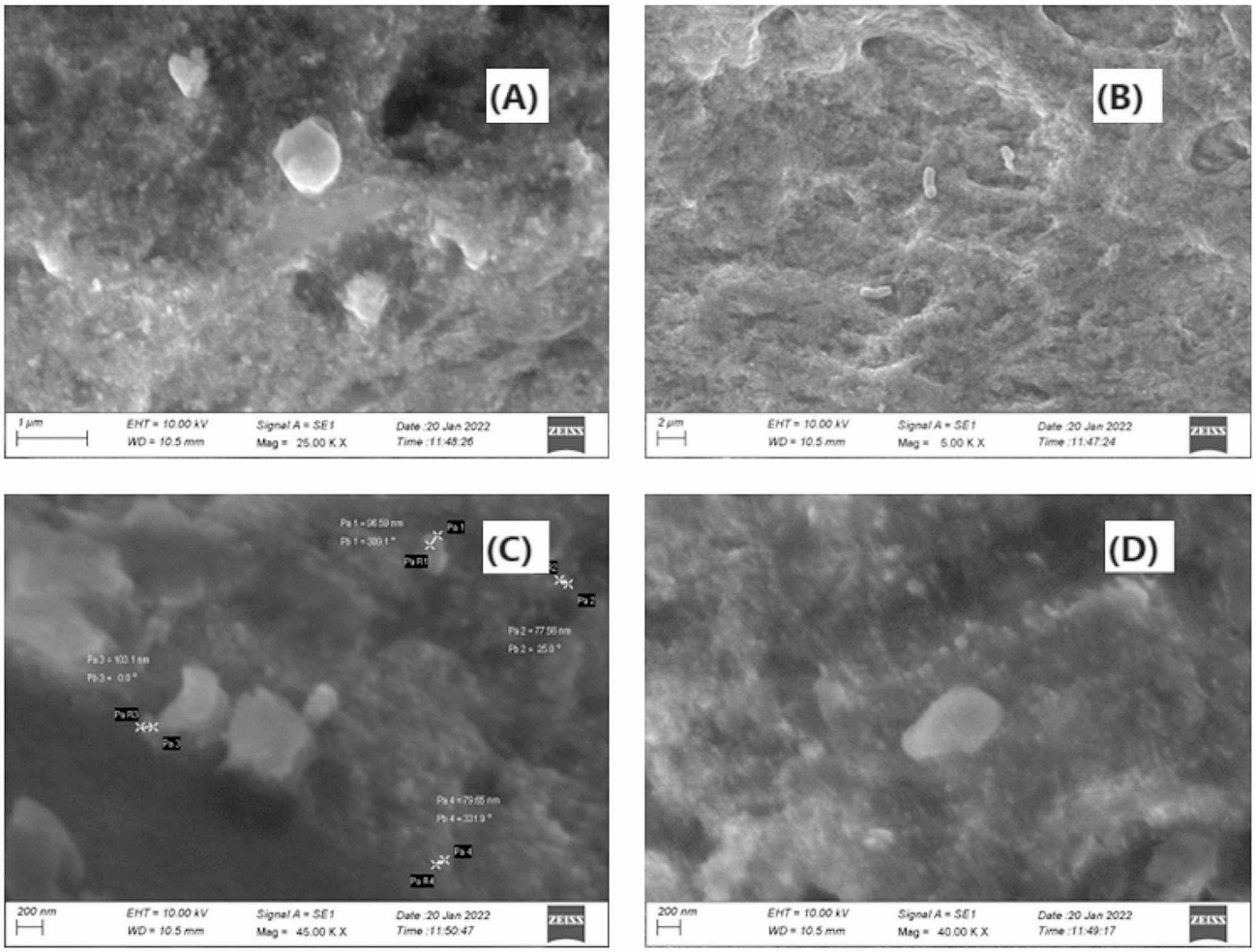

Fig. 5 Field emission scanning electron microscopy (FE-SEM) images of NS-AgNPs in different magnification for surface morphology identification

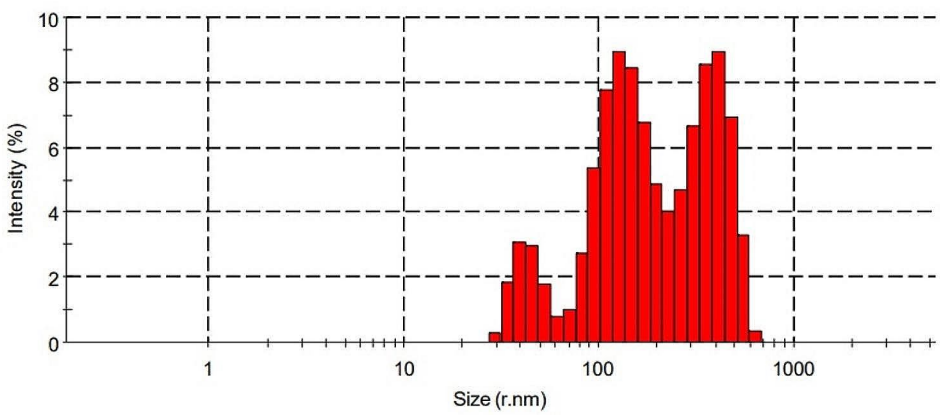

Fig. 6 DLS particles size distribution analysis of NS-AgNPs.

no agglomerates were observed until one hour. The Zeta potential value of the bioactive NS-Ag NPs in aqueous solution (Fig. 7) was observed to be −0.168 mV. It is a suitable surface charge for the potential cellular penetration of bacterial cells and the endocytosis mechanism of A549 lung cancer cells [20–22].

3.5 Antimicrobial Activity of NS-Ag NPs Against Human Pathogens

The antimicrobial effect of silver nanoparticles synthesized by *N. solani* (NS-AgNPs) are shown in Fig. 8 and were tested against human pathogens like *S. typhi, S. aureus, E. coli* and

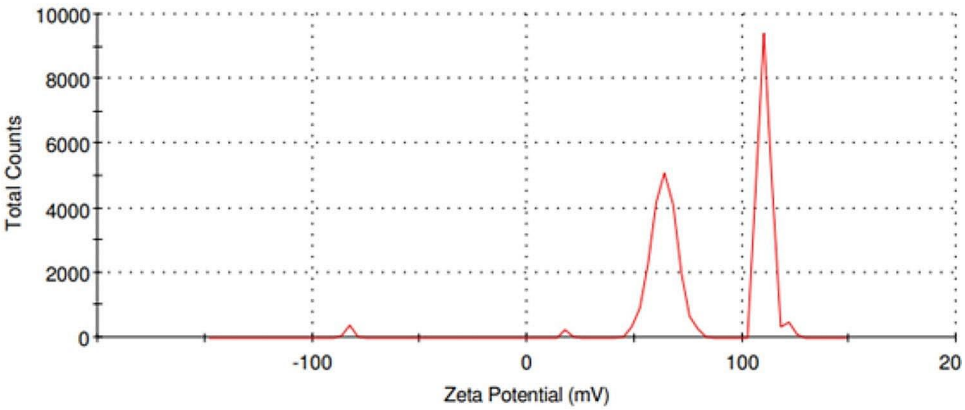

Fig. 7 Zeta potential analysis of NS-AgNPs using nano zeta analyser

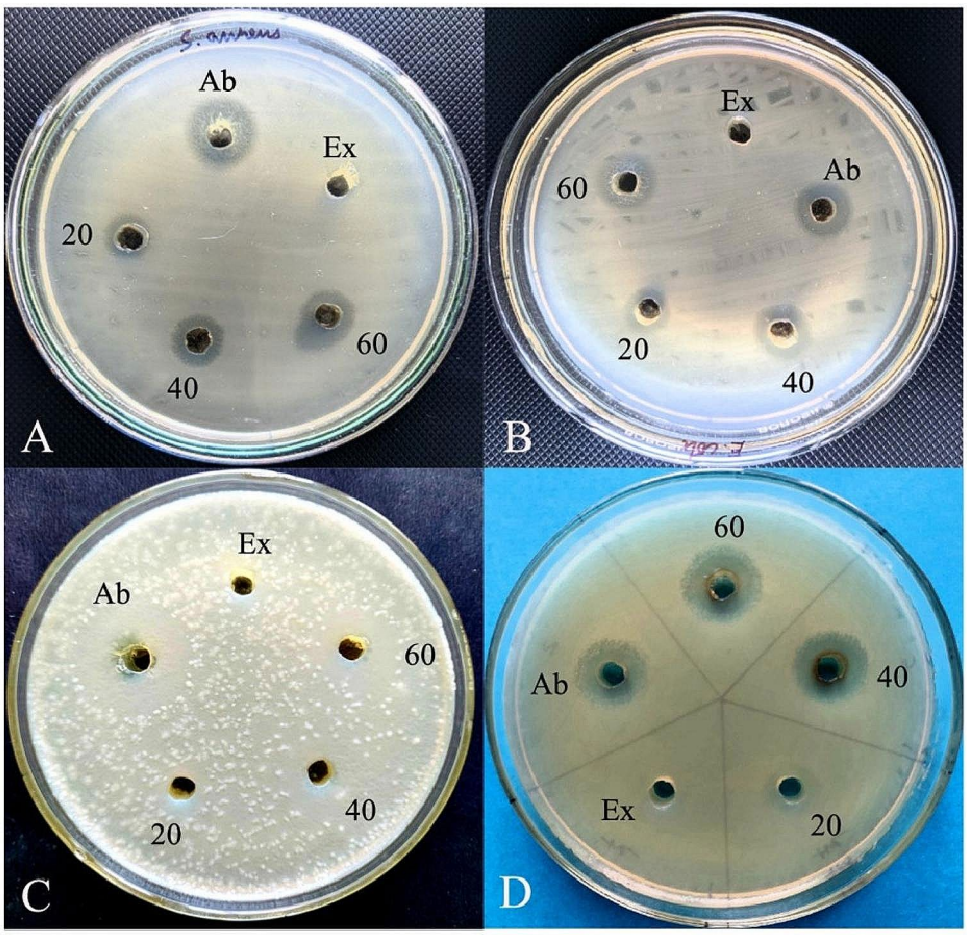

Fig. 8 Assessment of antibacterial potential of NS-AgNPs against human infectious pathogens using well diffusion assay with various concentrations. (**A**) *Staphylococcus aureus*; (**B**) *Escherichia coli*, (**C**) *Salmonella typhi*; (**D**) *Bacillus subtilis*. The NS-AgNPs concentration was 20, 40, 60 µg mL, respectively. Ab: standard antibiotic Streptomycin sulfate (10 µg well)

Table 1 Antibacterial activity of NS-AgNPs against human pathogens

Bacterial strains	Zone of inhibition (mm) / Sample concentrations (µg mL)				
	20	40	60	Positive control (10 µg mL)	NS extract
Staphylococcus aureus	7	12	13	15	0
Escherichia coli	8	13	12	16	0
Salmonella typhi	10	12	16	16	0
Bacillus subtilis	9	13	14	21	0

Values are presented in average ($n = 3$), Positive control-Streptomycin

B. subtilis. Synthesized NS-AgNPs show higher inhibitory action when compared to fungal extract. The anti-bacterial efficacy of NS-AgNPs was assessed by agar well diffusion assay. Results show a significant growth reduction against human pathogenic bacteria at minimum doses. The highest bacterial colony reduction was observed against *Salmonella typhi* (16 mm) at 60 µL concentration (Table 1). Increasing the concentration of NS-AgNPs enhances the bacterial zone of inhibition (Fig. 8). The results show that lower doses result in a considerable amount of bacterial zone of inhibition. The antibacterial efficacy of NS-AgNPs might be due interaction of silver ions and bioactive molecules released from fungal extract [16, 22, 27, 28]. The nanoscale AgNPs can easily penetrate into the bacterial cell wall. The presence of AgNPs has induced ROS-mediated cell dysfunctions [8, 9, 14, 16, 18]. Overall results revealed that biogenic synthesized NS-AgNPs are an effective antibacterial agent for bacterial infection control. The simultaneous release of silver and fungal extracellular bioactive compounds increased the suppression of bacterial growth at low levels [9, 16, 21].

3.6 Cytotoxicity Studies

The sample of the NS-AgNPs demonstrated considerable cytotoxicity against human lung cancer A549 cell lines at various doses. In this study, there was a dose-dependent cytotoxic response occurred with A549 lung cancer cells at higher concentrations (Fig. 9). The complete cell mortality rate of 95% of cell death was observed in 100 µg mL concentration of synthesized silver nanoparticles (NS-AgNPs). The IC_{50} concentration of NS-AgNPs against A549 lung cancer cells after 48 h treatment is 46.32 ± 1.02 µg mL. Hence, the presence of 100 µg mL of colloid NS-AgNPs significantly inhibits cell growth by more than 98% (Fig. 9). The results suggested that the synthesis of *Anaphalis contorta* entophytic fungi-mediated Ag nanoparticles own a great selectivity to cancer cells. If will be an effective material for cancer therapy. In addition, silver nanoparticles exhibit strong anticancer efficacy with minimal toxicity, depending on the reducing and capping agents used to convert silver nitrate into silver [14, 29].

3.7 Nuclear Damage Assessment

The apoptotic mechanism plays a vital role in cell morphology and biochemical changes [25]. The cytotoxic effect of bioactive NS-AgNPs leading to nuclear damage and cellular changes was evaluated by the Hoechst 33,342 staining method (Fig. 10). The quantitative percentage of normal/abnormal cell nuclei of the concentration of NS-AgNPs at 25 µg mL and 50 µg mL shows excellent nuclear damages and cell count reductions. The bioactive NS-AgNPs treated A549 cells showed 57.13 ± 0.14 and 73.22 ± 0.13% of abnormal nuclei. The control cells without treatment of NS-AgNPs exhibit only 4.3 ± 0.14% of abnormal nuclei. The microscopic image of control cells revealed that, the high level of normal cell nuclei with less blue fluorescence intensity. In this contest, NS-AgNPs treated cells exhibit excellent bright blue fluorescent with cytological changes in A549 cells with chromatin fragmentation, irregular nuclear structure, binucleation, and nuclei shrinkages (Fig. 10). The intra-cellular changes of NS-AgNPs treated cells illustrate the fact that the apoptosis process mediated cell death [29, 30]. The final results of Hoechst's staining assay suggest that significant death of A549 cells is reflected by the cytotoxic potential of Ag nanoparticles.

3.8 Bioactive NS-Ag NPs Mediated Apoptosis in A549 Lung Cancer Cells

The apoptosis mechanism of bioactive NS-AgNPs and changes in cell morphology were investigated via the AO/EB dual staining technique. Post-exposure to fungal extract-mediated AgNPs caused significant levels of morphological and nuclear changes against A549 lung cancer cells. In control cells there is no structural and nuclear deformities have occurred (Fig. 11). In this staining technique, live cells brightly emit green fluorescence and are distinguished from the apoptotic cells. After NS-AgNPs treatment, the microscopic images of a treated group exhibit a significant amount of reduction in live cells. Red cells were only observed in the concentration of 50 µg mL treatment. The percentage of apoptotic cells was increased after 24 h post-exposure. These AO/EB dual staining assay results indicate that A549 cell death after NS-AgNPs treatment occurred via the apoptosis mechanism [27, 28].

Conclusively, there are a variety of research works that demonstrate bioactive AgNPs synthesis and biomedical applications. Recently, endophytic fungal extract-mediated

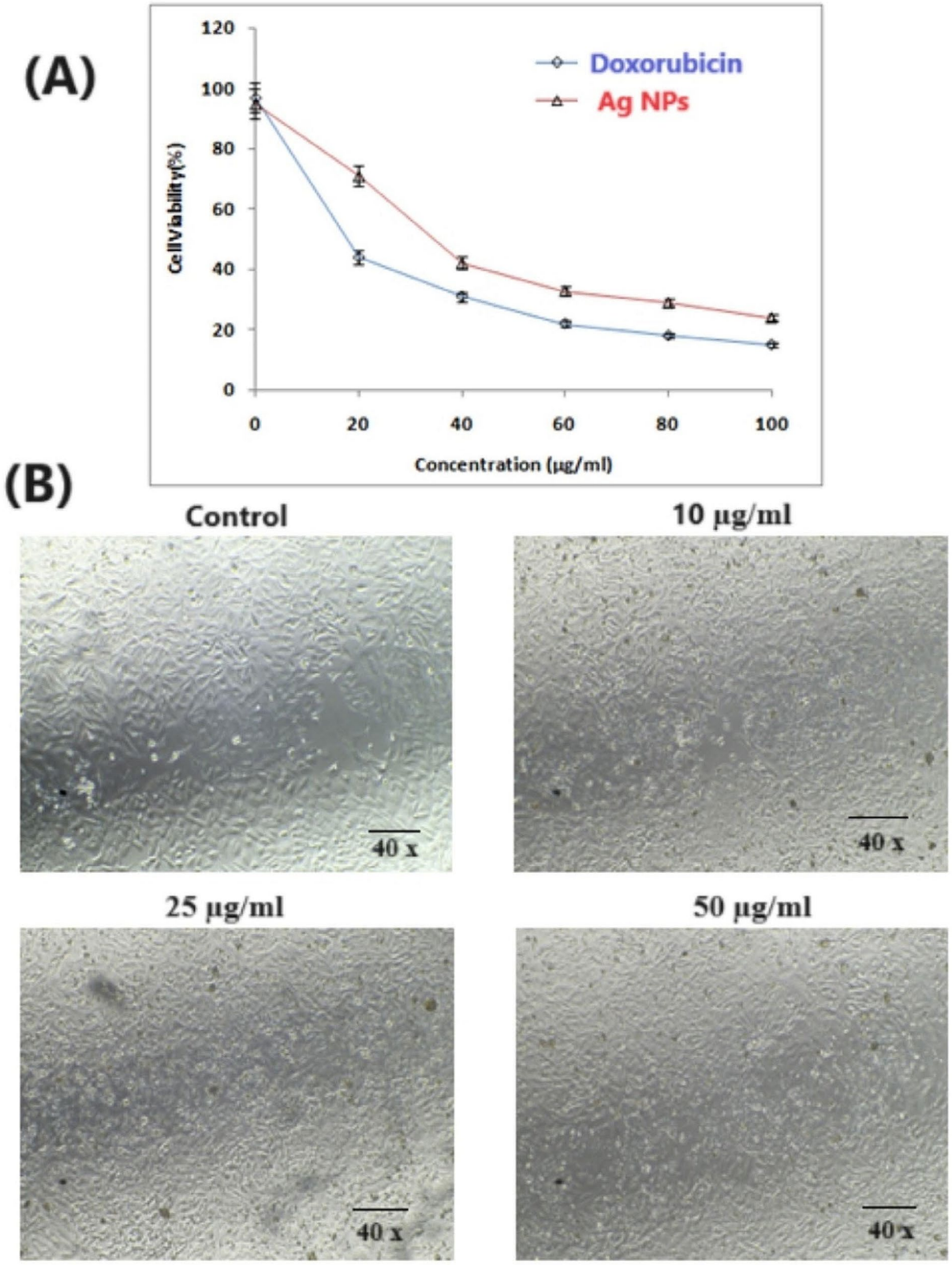

Fig. 9 (**A**) Cytotoxic effect of NS mediated AgNPs against A549 cells using MTT assay, (**B**) Phase contrast microscopic images of A549 cells after NS-Ag NPs treatment. The images were captured at 40 x magnification

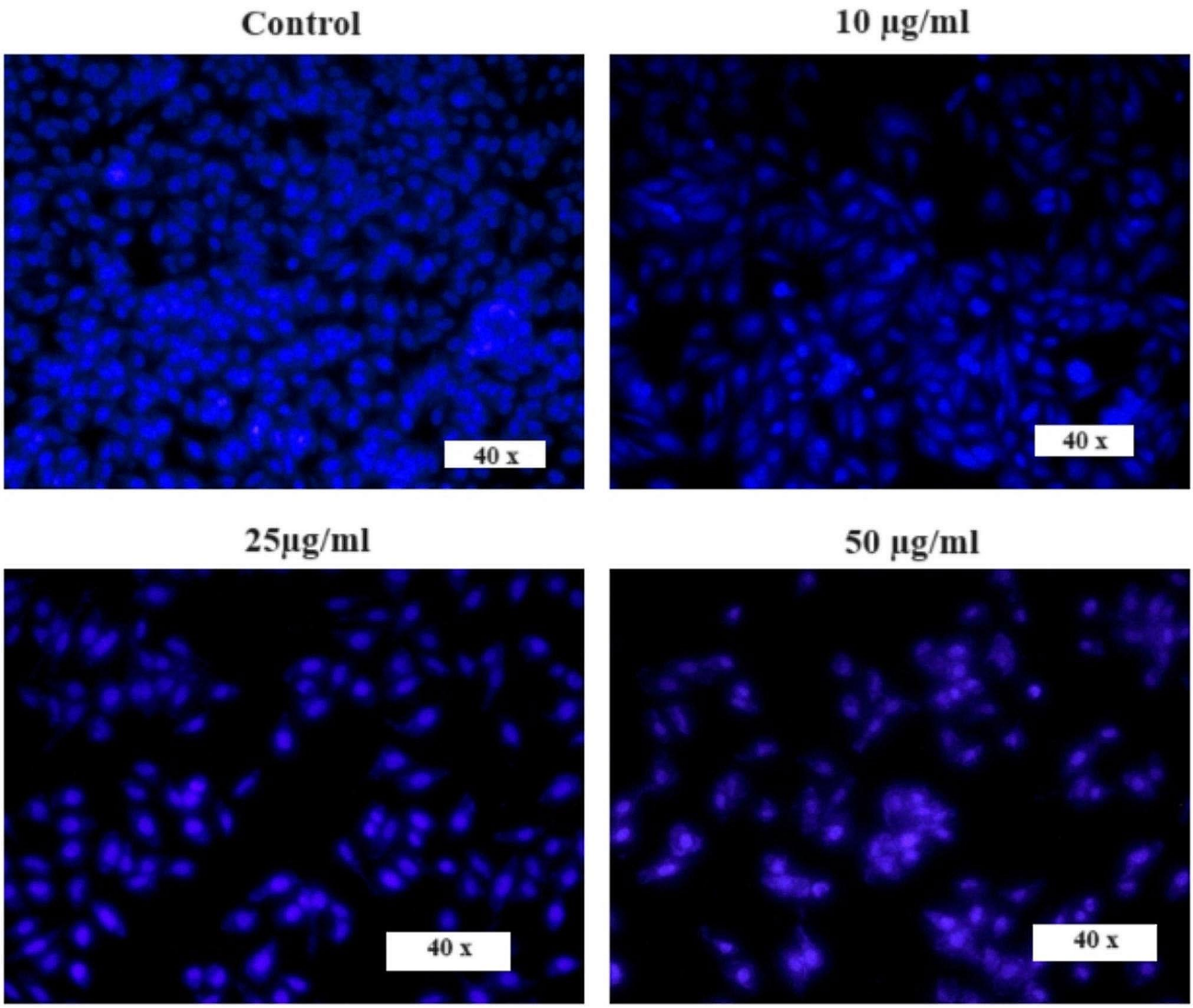

Fig. 10 Fluorescence microscopic images of A549 lung cancer cells after treatment of bioactive NS-AgNPs with Hoechst fluorescence staining at 40 x magnification

nanoparticles utilized to develop new efficient antibiotic and anticancer agents due to their biological characteristics. The preparation of fungal extract-mediated nanoparticles is also proposed to be safe for living cells [26]. However, the minimum amount of research work has been reported in endophytic fungi-mediated Ag nanoparticles synthesis and anticancer applications. The present in vitro anticancer and antibacterial experiments motivate new research for the possibility of bioactive Ag nanoparticles in the human health care sector. Treatment of Ag nanoparticles potentially eradicates the multiplication of infectious human pathogens. Over the result of this study revealed that bioactive Ag nanoparticles can be an effective material for pharmaceutical industries and are non-toxic to humans as compared to commercial antibiotics. The bioactive Ag nanoparticles exhibit a promising cytotoxic effect against A549 lung cancer cells. It will be an outstanding and effective material for lung cancer treatment after the clinical trials.

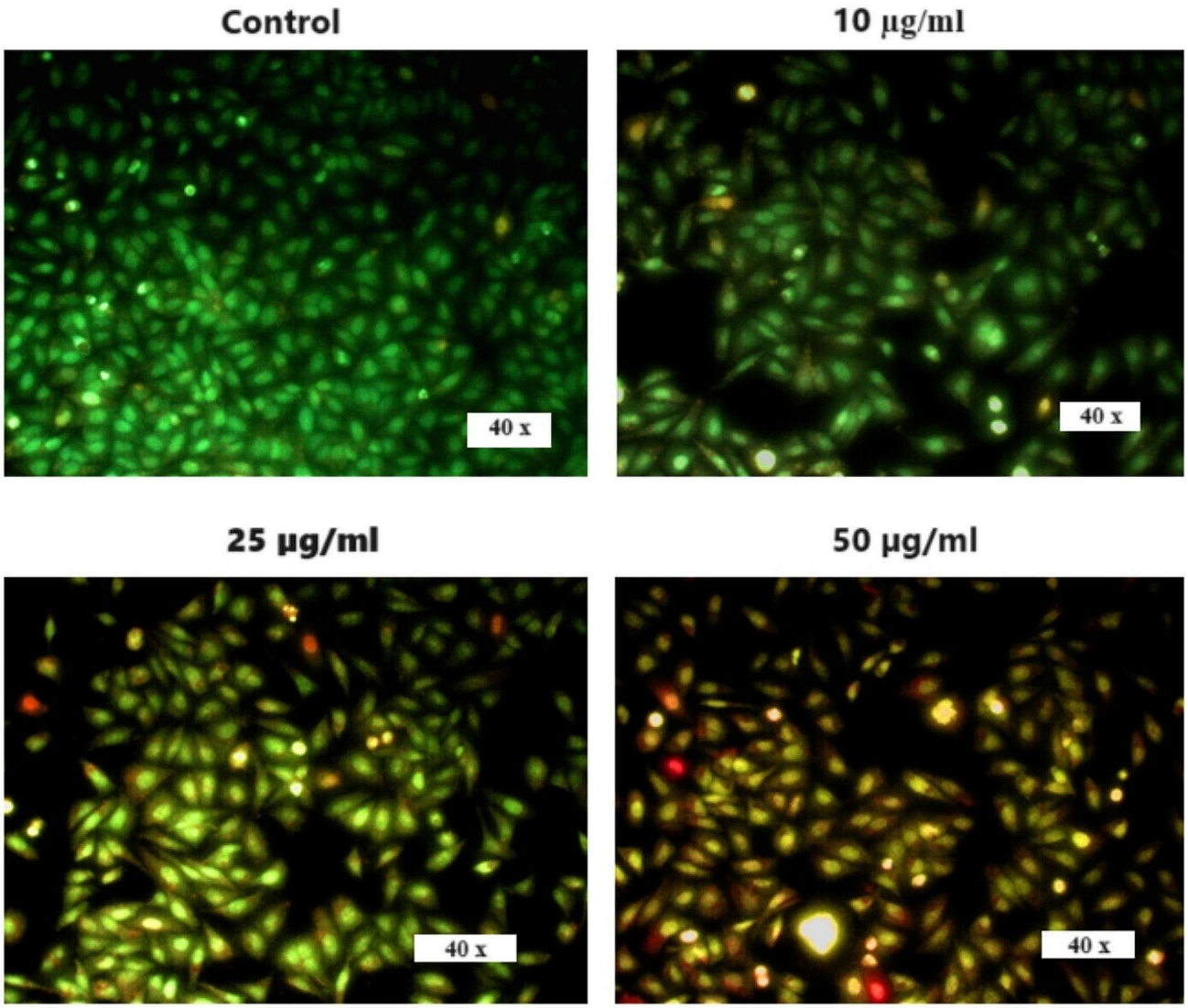

Fig. 11 Fluorescence microscopic images of A549 lung cancer cells after treatment of bioactive NS-AgNPs with AO/EB fluorescence staining at 40 x magnification

Acknowledgments The author (KSN) wishes to express his gratitude to the Head of the Department of Life Sciences (Botany), Manipur University, for providing lab space for his Ph.D. research.

Author Contributions The authors, K.S.N. and S.K., participated equally to this work by carrying out work, drafting the paper, reviewing, and editing. S.S.M. and R.R.P. proposed the idea, outlined the work, validated the results, and revised the manuscript. P.R. and L.G. assisted in the validation of the results, software, data curation, and authoring the original publication. All authors have reviewed and approved the manuscript.

Funding The author(s) received no financial support for the authorship, and/or publication of this article.

Data Availability No datasets were generated or analysed during the current study.

Declarations

Competing Interests The authors declare no competing interests. This article does not contain any studies with human participants or animals performed by any of the authors.

References

1. P. Mathur, K. Sathishkumar, M. Chaturvedi, P. Das, K.L. Sudarshan, S. Santhappan, ICMR-NCDIR-NCRP Investigator Group. Cancer statistics 2020: report from National Cancer Registry Programme, India. JCO Glob Oncol. **6**, 1063–1075 (2020)
2. S. Sharma, L. Satyanarayana, S. Asthana, K.K. Shivalingesh, B.S. Goutham, S. Ramachandra, Oral cancer statistics in India on the basis of first report of 29 population-based cancer registries. J. Oral Maxillofac. Pathol. **22**(1), 18–26 (2018)

3. R.L. Siegel, A.N. Giaquinto, A. Jemal, Cancer statistics 2024. CA Cancer J. Clin. **74**(1), 12–49 (2024)
4. S.M. Abdel-Aziz, R. Prasad, A.A. Hamed, M. Abdelraof, (2018) Fungal nanoparticles: a novel tool for a green biotechnology? *Fungal Nanobionics: Principles and Applications*. Springer, 61–87. https://doi.org/10.1007/978-981-10-8666-3_3
5. M. Goel, A. Sharma, B. Sharma, Recent advances in biogenic silver nanoparticles for their biomedical applications. Sustain. Chem. **4**(1), 61–94 (2023)
6. S. Husain, A. Nandi, F.Z. Simnani, U. Saha, A. Ghosh, A. Sinha, S.K. Verma, Emerging trends in advanced translational applications of silver nanoparticles: a progressing dawn of nanotechnology. J. Funct. Biomater. **14**(1), 47 (2023)
7. P.R. More, S. Pandit, A.D. Filippis, G. Franci, I. Mijakovic, M. Galdiero, Silver nanoparticles: bactericidal and mechanistic approach against drug resistant pathogens. Microorganisms. **11**(2), 369 (2023)
8. E. Alhomaidi, S.A. Jasim, H.I.M. Amin, M.A. Lima Nobre, M. Khatami, A.T. Jalil, S. Hussain Dilfy, Biosynthesis of silver nanoparticles using *Lawsonia inermis* and their biomedical application. IET Nanobiotech. **16**(7–8), 284–294 (2022)
9. S.E. Hammad, M.N. El-Rouby, M.M. Abdel-Aziz, G.S. El-Sayyad, H.H. Elshikh, (2023) Endophytic fungi–assisted biomass synthesis of gold, and zinc oxide nanoparticles for increasing antibacterial, and anticancer activities. Biomass Convers. Biorefin 1–18
10. R.J. Rodriguez, J.F. Jr White, A.E. Arnold, A.R.A. Redman, Fungal endophytes: diversity and functional roles. New. Phytol. **182**(2), 314–330 (2009). https://doi.org/10.1111/j.1469-8137.2009.02773.x
11. K.S. Nongthombam, S.S. Mutum, R.R. Pandey, (2024) *In Vitro* Biological activities of an endophytic fungus, *Trichoderma* sp. L2D2 isolated from *Anaphalis Contorta*. Indian J. Microbiol. 1–12
12. K.S. Nongthombam, S.S. Mutum, R.R. Pandey, Secondary metabolite profiling of the endophytic fungus *Trichoderma longibrachiatum* L2D2 isolated from *Anaphalis Contorta*. Annu. res. rev. biol. **39**(2), 1–15 (2024)
13. R.K. Joshi, *In vitro* antimicrobial activity of the essential oil of *Anaphalis contorta* hook f. Int. J. Res. Pure Appl. Micro. **1**(2), 19–21 (2011)
14. S. Abdel-Hafez, N.A. Nafady, I.R. Abdel-Rahim, A.M. Shaltout, M.A. Mohamed, Biogenesis and optimisation of silver nanoparticles by the endophytic fungus *Cladosporium sphaerospermum*. Int. J. Nano Chem. **2**(1), 11–19 (2016). https://doi.org/10.18576/ijnc/020103
15. P. Tripathy, S. Sethi, D. Panchal, O. Prakash, A. Sharma, R.B. Mondal, S. Pal, (2023) Biogenic synthesis of nanoparticles by amalgamating microbial endophytes: potential environmental applications and future perspectives. *Microbial Endophytes and Plant Growth*. Academic 215–231
16. E. Saied, M.A. Abdel-Maksoud, A.A. Alfuraydi, M. Bassyouni, A.H. Hashem, Endophytic *aspergillus hiratsukae* mediated biosynthesis of silver nanoparticles and their antimicrobial and photocatalytic activities. Front. Microbiol. **15**, 1345423 (2024)
17. K. Bloch, S. Ghosh, *Endophytic fungi-mediated Synthesis of gold and Silver Nanoparticles* (What, Why and How? Academic, In: Endophytic Association, 2023), pp. 19–36
18. S.A. Gezaf, H.A. Hamedo, A.A. Ibrahim, M.I. Mossa, Mycosynthesis of silver nanoparticles by endophytic Fungi: mechanism, characterization techniques and their applications. Micro Biosyst. **7**(2), 48–65 (2022)
19. W.S. Devi, K. Surendirakumar, M.S. Singh, Distribution of endophytic fungi associated with *Meriandra Bengalensis* Benth. And assessment of their bioactive potential in vitro. Vegetos. **35**(4), 995–1006 (2022)
20. A. Sharma, A. Sagar, J. Rana, R. Rani, (2022) Green synthesis of silver nanoparticles and its antibacterial activity using fungus *Talaromyces purpureogenus* isolated from *Taxus baccata* Linn. *Micro and Nano Syst Lett* 10(2) https://doi.org/10.1186/s40486-022-00144-9
21. G. Lakshmanan, A. Sathiyaseelan, P.T. Kalaichelvan, K. Murugesan, Plant mediated synthesis of silver nanoparticles using fruit extract of *Cleome viscosa* L.: assessment of their antibacterial and anticancer activity, Karbala Inter. J. Mod. Sci. **4**(1), 61–68 (2018)
22. S. Anbazhagan, S. Azeez, G. Morukattu, R. Rajan, K. Venkatesan, K.P. Thangavelu, Synthesis, characterization and biological applications of mycosynthesized silver nanoparticles. 3 Biotech. **7**, 1–9 (2017)
23. M.E. Rabab, E.A. Raida, A.H. Awatif, Biosynthesis and characterization of silver nanoparticles using *Trichoderma longibrachiatum* and their effect on phytopathogenic fungi. EJBPC **28**, 28 (2018). https://doi.org/10.1186/s41938-018-0028-1
24. P. Raju, K. Balakrishnan, M. Mishra, T. Ramasamy, S. Natarajan, Fabrication of pH responsive FU@ Eu-MOF nanoscale metal organic frameworks for lung cancer therapy. J. Drug Deliv Sci. Technol. **70**, 103223 (2022)
25. K. Saravanakumar, S. Shanmugam, N.B. Varukattu, D. MubarakAli, K. Kathiresan, M.H. Wang, Biosynthesis and characterization of copper oxide nanoparticles from indigenous fungi and its effect of photothermolysis on human lung carcinoma. J. Photochem. Photobiol B **190**, 103–109 (2019)
26. M. Rudrappa, R.S. Kumar, S.K. Nagaraja, H. Hiremath, P.V. Gunagambhire, A.I. Almansour, K. Perumal, S. Nayaka, Myconanofabrication of silver nanoparticles by *Penicillium Brasilianum* NP5 and their antimicrobial, photoprotective and anticancer effect on MDA-MB-231 breast cancer cell line. Antibiotics. **12**(3), 567 (2023). https://doi.org/10.3390/antibiotics12030567
27. M.K. Sangeeta, V.M. Tejashree, Gunagambhire, M.P. Bhat, S.K. Nagaraja, P.V. Gunagambhire, R.S. Kumar, S.M. Mahalingam, In-vitro evaluation of *Talaromyces Islandicus* mediated Zinc Oxide nanoparticles for Antibacterial, Anti-inflammatory, bio-pesticidal and seed growth promoting activities. Waste Biomass Valoriz. **15**, 1901–1915 (2024). https://doi.org/10.1007/s12649-023-02386-z
28. M.P. Bhat, B. Chakraborty, S.K. Nagaraja, P.V. Gunagambhire, R.S. Kumar, S. Nayaka, A.I. Almansour, K. Perumal, *Aspergillus niger* CJ6 extract with antimicrobial potential promotes *in-vitro* cytotoxicity and induced apoptosis against MIA PaCa-2 cell line. Environ. Res. **229**, 116008 (2023)
29. M. Rudrappa, R.S. Kumar, D.S. Basavarajappa, M.P. Bhat, S.K. Nagaraja, A.I. Almansour, K. Perumal, S. Nayaka, *Penicillium citrinum* NP4 mediated production, extraction, physicochemical characterization of the melanin, and its anticancer, apoptotic, photoprotection properties. Int. J. Biol. Macromol. **245**, 125547 (2023)
30. S.K. Nagaraja, S.K. Niazi, A. Bepari, R.A. Assiri, S. Nayaka, *Leonotis nepetifolia* flower bud extract mediated green synthesis of silver nanoparticles, their characterization, and in vitro evaluation of biological applications. Materials. **15**(24), 8990 (2022)

Publisher's Note Springer Nature remains neutral with regard to jurisdictional claims in published maps and institutional affiliations.

Springer Nature or its licensor (e.g. a society or other partner) holds exclusive rights to this article under a publishing agreement with the author(s) or other rightsholder(s); author self-archiving of the accepted manuscript version of this article is solely governed by the terms of such publishing agreement and applicable law.